O. C. Iloeje[1]
Lecturer,
University of Nigeria,
Nsukka,
Anambra State, Nigeria

J. A. Kervinen
Engineer.

J. Ireland
Engineer.

B. S. Shiralkar
Manager.

ECCS Methods,
General Electric
Nuclear Energy Division,
San Jose, Calif.

Flow Split Relationships in Two-Phase Parallel Channel Flows

The observed flow combinations through the channels were: cocurrent upflow in both channels, cocurrent upflow in one and countercurrent flow in the other channel, and cocurrent upflow in one and single phase liquid downflow in the other channel. The flow regimes in each channel varied from churn-turbulent, through anular flow, to chugging counter-current flow, as the flow conditions were varied. It was observed that the flow combination obtained was history dependent. However, for given flow combinations, certain flow split relationships were established. With both channels in cocurrent upflow, the flow quality into each channel was approximately the same as the flow quality in the lower plenum at the flow split elevation. For the other flow combinations, a simple relationship between the void fractions at the bottom of the channels which had two phase fluid, and the average void fraction and vapour flux in the lower plenum at the flow split elevation, was established.

Introduction

In the analysis of the thermal-hydraulic response of a Nuclear Reactor (BWR or PWR), during loss of coolant accidents, it is necessary to know the phase flow rates through each bundle so that an accurate fuel cladding heat-up transient can be calculated. A similar need is encountered in process industries when a two-phase mixture flows from a common inlet header (plenum) through multiple parallel channels, to a common exit header. The flow rates through each channel will depend on the homogeneity of the inlet flows, the pressure drop characteristics of the channels, and the conditions of energy and mass transfers inside the channels. If the inlet flow is homogeneous and the channel conditions are identical, then the phase flows may be assumed equally split among the channels. Generally, this is not the case, and an involved model is required to calculate the different flows.

Figure 1 shows a possible flow configuration for a set of vertical, parallel dissimilar channels. The configuration shows some channels in cocurrent upflow, and others in countercurrent flow or single phase flow at the bottom entry. There is an equally mixed flow mode at the top exit of the channels. Obviously an equal flow split among the channels cannot be assumed. If the channels and plena are assumed to be one dimensional flow paths in which pressure variations across a given elevation are negligible, then it may be assumed that the pressure drop across each channel is the same. This gives a set of equations for determining the phase flows into the channels. Additional equations are obtained from the conservation of mass and energy.

It can be shown that a total of $(5N+1)$ equations will be obtained from the above relationships, in terms of W_{g0}, W_{f0}, P, Q_i, W_{gi}^b, W_{fi}^b, W_{gi}^t, W_{fi}^t, ΔP_i, and θ_i. N is the total number of channels. With W_{g0}, W_{f0}, P, and Q_i as the known quantities, there are $6N$ unknowns. The additional $N-1$

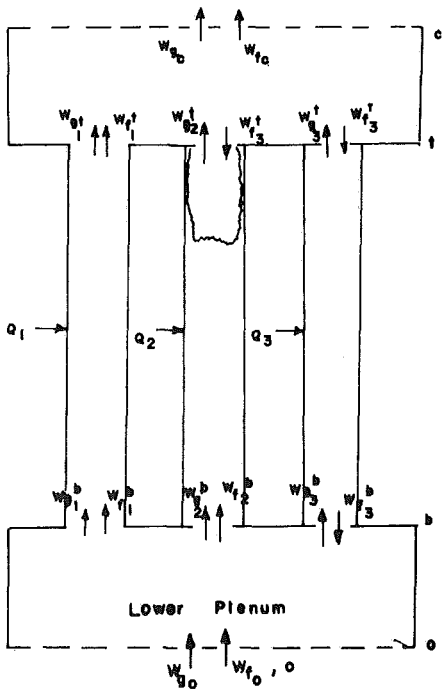

Fig. 1 Parallel channels with mixed mode flow

[1] Formerly Senior Engineer, General Electric Nuclear Energy Division, San Jose, Calif.

Contributed by the Fluids Engineering Division for publication in the JOURNAL OF FLUIDS ENGINEERING. Manuscript received by the Fluids Engineering Division, November 14, 1980.

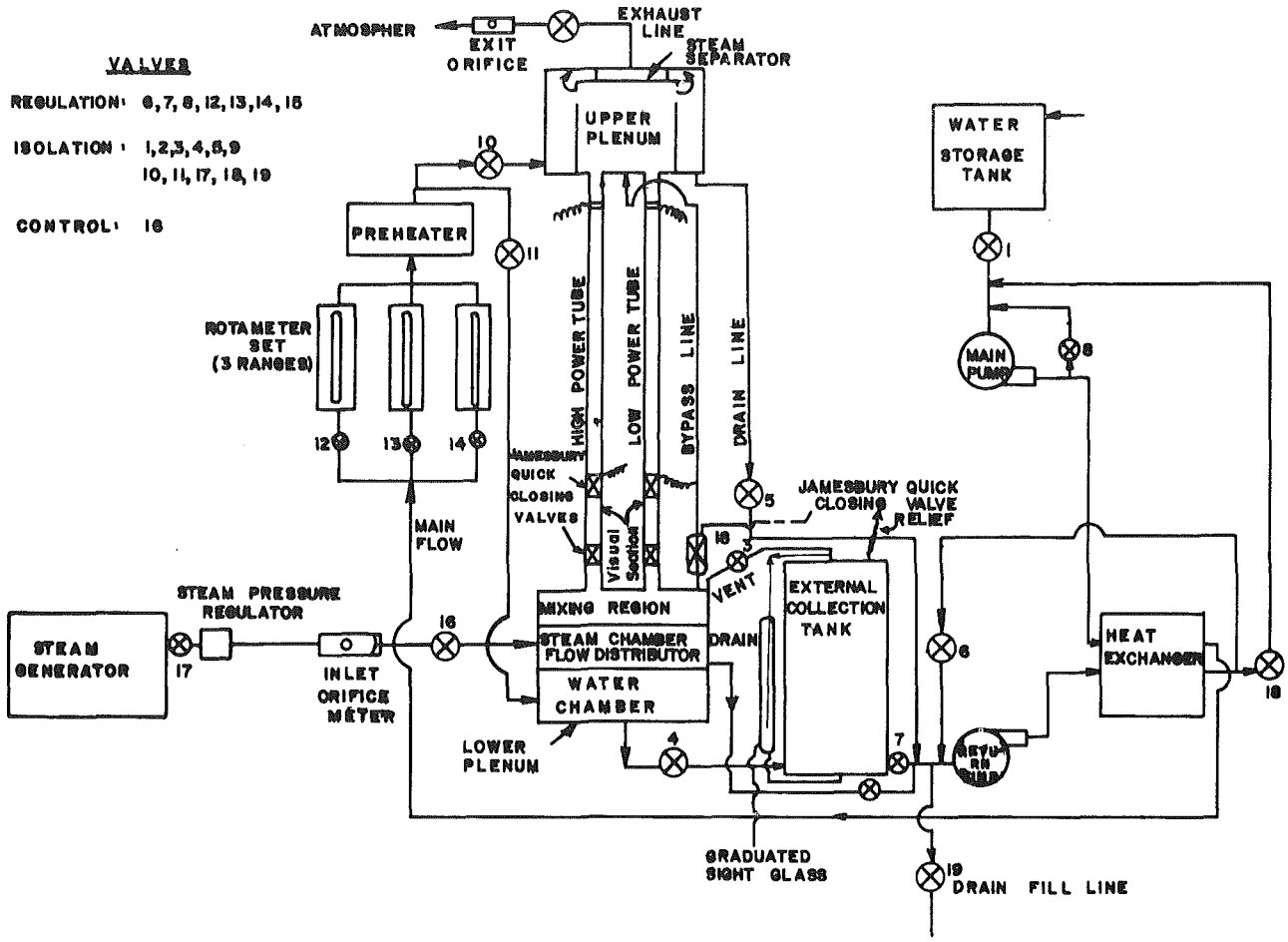

Fig. 2 Sketch of test loop

equations required can be supplied by specifying relationships between the liquid and vapor flows at the entries or exists to $(N-1)$ channels. Since these relationships are usually not known in the general case, and there's a high degree of uncertainty as to their assumption, an experimental programme was therefore set up to determine them.

Some Relevant Previous Work

Eselgroth and Griffith [1] studied the steady state flow configurations for five parallel tubes, using freon and blocked plena inlets. The authors, as in this paper, observed cocurrent up flow and countercurrent flow in the tubes. They concluded that cocurrent downflow was not possible. This conclusion may not hold in all cases. Countercurrent flow limitation (CCFL) at the upper orifices of some high power channels, or the introduction of subcooled liquid into some vapor filled channels, during a reflood transient, may cause most of the reflood liquid to flow down a few channels. The resulting high liquid velocities may cause transient cocurrent downflows. The effects of liquid subcool on parallel channel behaviour was studied in reference [2].

Reference [3] demonstrated that single tube data could be used to predict burnout, flow reversal points, and single phase liquid flow rates into a five channel array, with blocked inlets. There was no need for phase split relationships. Reference [4] presented a model for calculating two phase flow split transients (including flow reversals) for parallel channels. Single tube pressure drop correlations, as well as history dependent phase split relationships, were used.

The Experiment

The objectives of the test were therefore,

(*a*) to determine the relationship(s), if any, between the two phase flow in the lower plenum and the phase flows at the bottom entry into the channels.

Nomenclature

P = pressure bar
W = flow rate kg/s
θ = vapor generation rate kg/s
Q = heat addition rate kW
X, x = quality
ϕ, α = void fraction
$h; h_{fg}$ = enthalpy; enthalpy of evaporation KJ/kg
A, a = flow area m^2
C_0 = void distribution parameter
g = vapor phase
f = liquid phase
$f0$ = total inlet liquid
$g0$ = total inlet vapor
hpt, HPT = high power tube – with 9.5mm inlet orifice
lpt, LPT = low power tube – with 6.4mm inlet orifice
ch = channel
lp = lower plenum
V_{gj} = slip velocity m/s
G = mass flux kg/s – m^2
Re = Reynolds number
$\rho; \sigma$ = density kg/m^3; surface tension N/m
Δ = finite change in given quantity

Subscripts and Superscripts

$i, 1, 2$ = channel identifier
$b; t$ = bottom; and top of channel, respectively

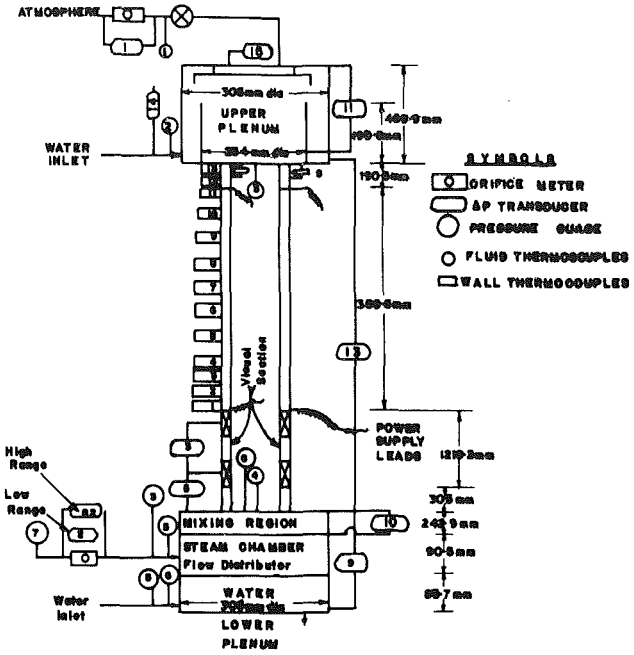

Fig. 3 Test section instrumentation (not to scale)

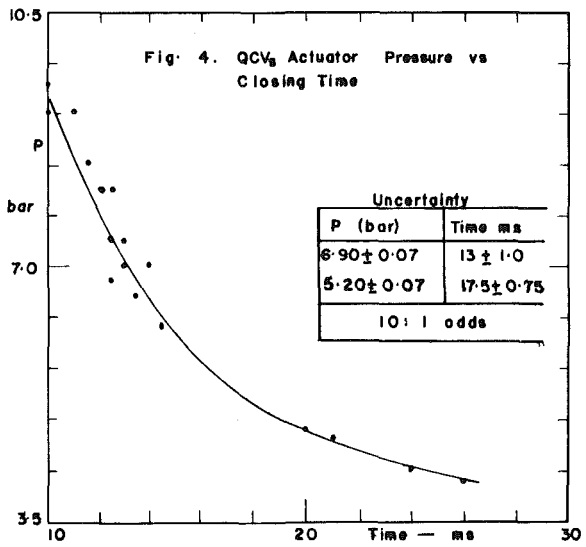

Fig. 4

(*b*) to determine the effects of test section power levels and power ratios, and methods of establishing the flows, on the relationship(s).

Test Loop. The test loop is sketched in Fig. 2. The loop includes a low pressure steam generator rated at 8.3 bar and 0.0378 kg/s. The steam passes through a pressure regulator, which maintains the downstream pressure at a preset value of 1.38 – 1.41 bar. It then flows into the steam side of the lower plenum flow distributor. The steam mixes with water in the upper region of the lower plenum, above the distributor, and the two phase mixture splits into the parallel tubes at phase ratios which depend on the flow conditions. In the upper plenum, the vapor flows around and over an inverted cup, which prevents liquid carry-over, before being exhausted into the atmosphere. The water returns through the drain line.

The water loop is a quasi-closed circuit, with make up water from the storage tank. The 33½ kW capacity preheater is used to bring the water to saturation before it flows into the upper or lower plenum, as required. Water, introduced into

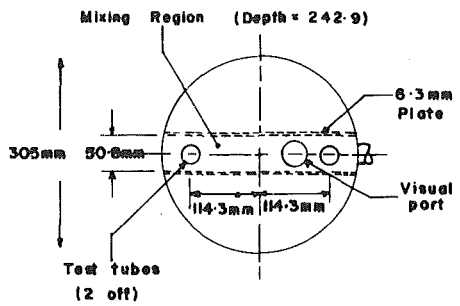

Fig. 5 Plan of lower plenum showing mixing region

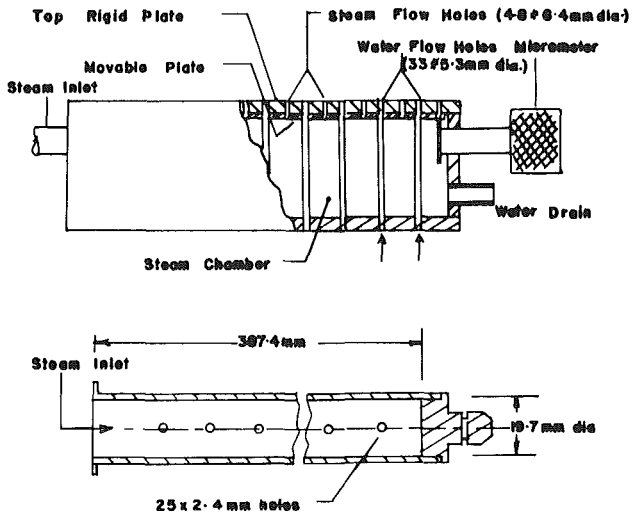

Fig. 6

the lower plenum, passes from the water side of the lower plenum flow distributor into the mixing region. The return flow from the upper plenum passes from the return pump back to the preheater. There is also a 0.283m^3 external collection tank, used in some experiments to measure the net amount of water draining from the channels into the lower plenum.

The test sections are two 5220mm long × 25.4 mm od × 23.6 mm id stainless steel tubes, instrumented as shown in Fig. 3. They can be electrical-resistance heated over approximately 3505mm of their lengths. Each tube has a 1219mm long visual section made of 23.6mm id pyrex tube, between the QCV's. The restriction at the bottom entry of the HPT is a 9.5mm square-edge orifice, and that for the LPT is a 6.4mm orifice of similar design. At the top exit of each tube is a 4-hole × 7.6mm orifice.

The four 25.4mm Jamesbury ball valves, which form part of the Quick Closing Valve system, are designed to close or open simultaneously. The closing time for the test was 13-14 milliseconds (actuator air pressure of 7 bar). A plot of air-pressure vs closing time is shown in Fig. 4. When actuated, the valves trap the fluid between them. After stratification the volume of liquid trapped between the QCV's, and hence the average void fraction between the valves, can be measured.

The outputs of the measuring instruments, in millivolts (except for the rotameters and pressure gauges) were recorded on a Dymec data acquisition system, and appropriately converted to actual units using the instruments caliberation curves.

The Mixing Region. The plan of the lower plenum, sketched in Fig. 5, shows the mixing region. It is a 50.8mm wide × 242.9mm deep section, running diametrically across

Table 2 Results for tests of Table 1

Run Number		38	39	40	3000	3024	1001	1004
W_g*10^3	HPT	5.71	4.95	5.66	1.17	5.30	4.94	4.81
kg/s	LPT	0.0	0.81	0.0	0.08	0.84	0.69	0.0
W_f*10^3	HPT	247.6	27.6	232.1	272.2	32.3	29.5	18.7
kg/s	LPT	−247.6	−27.6	−232.1	28.0	14.9	−29.5	−52.4
α between	HPT	.8055	.956	.8049	.6545	.9499	.9552	.9597
QCV's	LPT	0.0	.780	0.0	.6545	.9123	.7605	0.0
Inlet	HPT	.023	.152	.024	.0043	.141	.1436	.2048
Quality	LPT	0.0	–	0.0	.003	.0535	–	0.0
Lower Plenum	α	.4301	.4574	.4217	.185	.505	.4452	.4162
(top)	X	–	–	–	.004	.115	–	–
$\frac{1}{\alpha_{lp}} - \frac{1}{\alpha_{ch}}$	HPT	1.08	1.13	1.13	3.50	0.92	1.19	1.35
(α_{ch} at inlet)	LPT	–	1.19	–	3.22	0.86	1.25	–
$(\rho_g V_{gj}/G_g)_{lp}$		0.85	0.74	0.89	3.62	0.60	0.79	0.94

Table 1 Sample test matrix

Run number			W_{g0} $*10^3$kg/s	W_{f0} $*10^3$kg/s (net)	Test procedure	T Atm °C	P_{lp} bar	P test section bar
	HPT	LPT						
38	0.0	0.0	5.71	0.0	Gradual introduction of vapor	26	1.72	0.38
39	0.0	0.0	5.76	0.0	Sudden introduction of vapor	26	1.48	0.096
40	1.878	1.0	5.66	0.0	Gradual introduction of vapor	26	1.79	0.34
3000	3.612	2.025	1.25	300.26	Gradual introduction of liq. and vap. in LP	23.9	1.97	0.35
3024	3.60	1.975	6.14	47.14	Same as for 3000	23.9	1.67	0.24
1001	1.806	1.0	5.56	0.0	Gradual introduction of vapor	23.9	1.53	0.08
1004	1.758	1.0	4.82	−33.73	Same as for 1001 with net liquid downflow	23.9	1.57	0.165

the lower plenum. Liquid and vapor are introduced, through uniform distribution holes, into the bottom of the mixing region, and they flow out through the channels at the top of the region.

Flow Distributor. The two types of flow distributors used are shown in Fig. 6. The vapor hole size for type 1 (Runs 10 to 1012, and 3000 to 5026R) can be altered, using the movable plate. Type-2 (for Runs 1013 to 2017 and 9015) is a simple tube with holes drilled on its upper side.

Further details of the test section may be found in reference [5].

Experimental Procedure. In the tests, saturated vapor was always supplied to the lower plenum. Saturated liquid was supplied either to the lower plenum or to the upper plenum. In the former case, net cocurrent flow through the channels, were established. In the latter, net countercurrent flow or net zero liquid flow (liquid downflow in one channel = liquid upflow in the other channel) was established. For liquid supply to the upper plenum, the external collection tank was used to measure the net liquid downflow.

With the net liquid down flow as zero, the method of introducing the vapor was varied. In some of such runs, the vapor flow rate was gradually increased to the desired value. In others, the QCV's were closed while the vapor was introduced into the lower plenum. The lower plenum was thus pressurised. The QCV's were then opened, so that vapor was suddenly introduced into the channels. The flow rates were allowed to stabilize before data were taken.

At steady state, the transducer outputs were recorded on channels 1-62 of the Dymec over many cycles. The average values over the cycles were used. Pressure gauge and rotameter readings were manually taken. From these data, total liquid and vapor flow rates, test section powers, inlet void fractions, qualities, pressures, and pressure drops were calculated.

The tube/QCV system was calibrated for void/quality

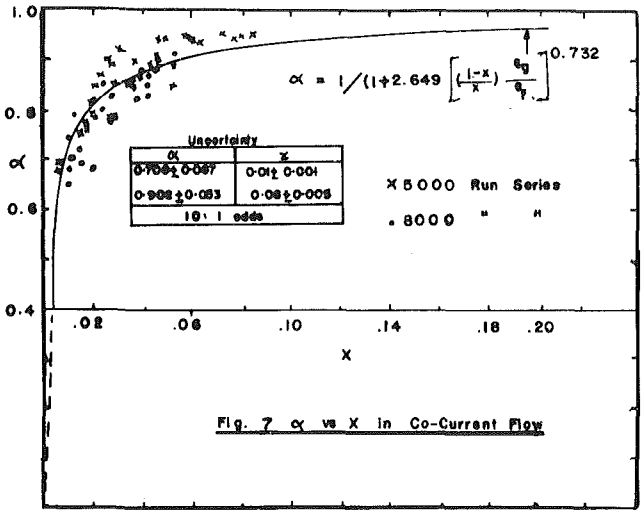

Fig. 7 α versus X in cocurrent flow

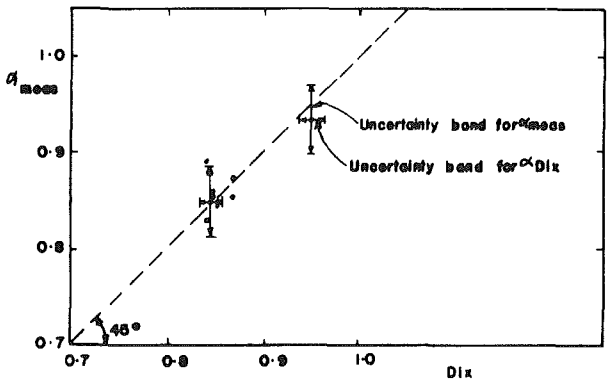

Fig. 8 α_{meas} versus α_{DIX} in chugging countercurrent flow

relations in cocurrent and counter-current flows, with one tube operating at a time.

Test Matrix. The flows and heat inputs varied within the following ranges:

W_{g0}: $1.26-129.8*10^{-3}$ kg/s; W_{f0}: (downflow) $0-472.5*10^{-3}$ kg/s

Q_{hpt}: $0-20.7$ KW; W_{f0}: (upflow) $0-504.9*10^{-3}$ kg/s

Q_{lpt}: $0-5.2$ KW; Q_{hpt}/Q_{lpt}: $1-1.8$

The test matrix for some representative tests is shown in Table 1, with the corresponding results shown in Table 2.

Data Reduction

Void Fraction and Flow Quality. The average void fraction between the QCV's is given by

$$\alpha = \frac{\text{Volume between QCV's} - \text{Volume of liquid trapped}}{\text{Volume between QCV's}} \quad (1)$$

If the flow is fully developed and there is negligible flashing or condensation of vapor between the QCV's, then the value of α given by equation (1) is also the value of the constant α between the QCV's.

Using Latzko's [6] expression for onset of fully developed turbulent velocity profile in single phase flow, (equation (2)), but with a two phase flow viscosity given by equation (3),

$$Z/D = 0.693\ \mathrm{Re}^{1/4} \quad (2)$$

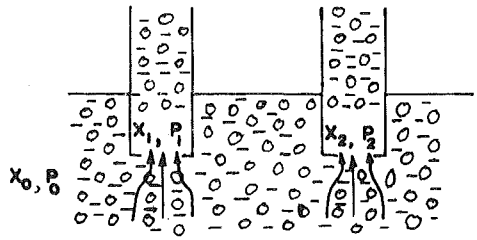

Fig. 9(*a*) All channel inlets and lower plenum in cocurrent up flow

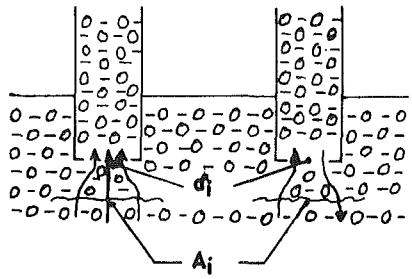

Fig. 9(*b*) Mixed flow modes at channel entries. All channel inlets submerged in two phase mixture in lower plenum

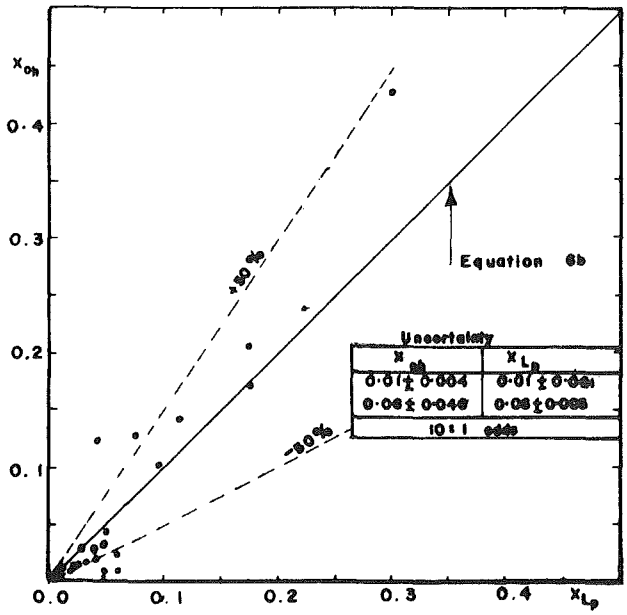

Fig. 10 X_{ch} versus X_{lp} for HPT

$$\mu = \chi\mu_g + (1-x)\mu_f \quad (3)$$

the largest Z/D for fully developed flow in the experiments was approximately 10. Allowing for an underestimate of 50 percent by equation (2), the value becomes 20. This gives a developing length of 472 mm. The length of tube between the lower plenum and the lowest QCV was 305 mm, or 13 diameters. Thus at highest flow rate, length of developing flow extending into the pyrex tube was 167 mm, or only 14 percent of the length of the pyrex tube. The flow was therefore assumed fully developed, or nearly so, at entry to the pyrex section.

The measured α corresponded to the actual α somewhere between the QCV's. Changes in vapor flow rate between the QCV's, though small, arose predominantly from gravity pressure changes. For a given test, this was approximately linear with height. For small changes in x and α, α would also vary approximately linearly with height. The measured average void fraction was therefore assumed to correspond to the actual α at the midpoint of the pyrex tube. Errors from

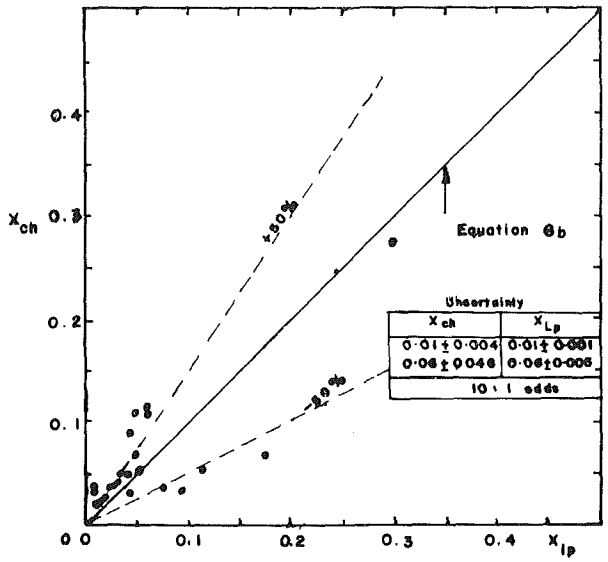

Fig. 11 X_{ch} versus X_{lp} for LPT

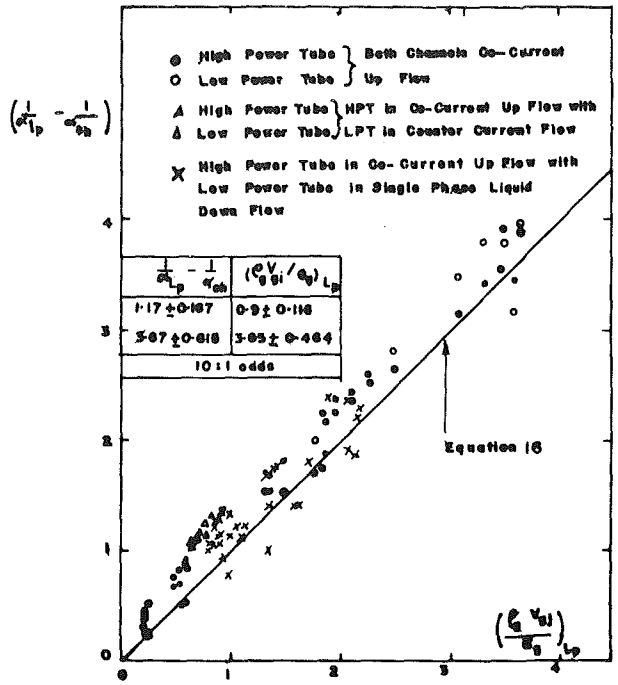

Fig. 12 Comparison of flow split data with equation (34) $(1/\alpha_{lp} - 1/\alpha_{ch})$ versus $(\rho_g V_{gj}/G_g)_{Lp}$

this assumption on the corresponding values of x were calculated and found negligible.

Flow quality, $W_g/(W_g + W_f)$, at entry to the channels differed from those within the pyrex tube, principally as a result of throttling at the inlet orifices. An energy equation between lower plenum and the midpoint of the pyrex tube was written to correct for the effects of pressure change, potential and kinetic energy changes and heat losses. The effects of the last three factors were very small.

Flow Split With Both Channels in Cocurrent Flow at Inlet. The phase flow rates, W_g and W_f at entry to each channel were determined using the mass conservation equations for liquid and vapor at lower plenum/channel boundary, void-quality relationship given in equation (4) and obtained from caliberation data, and the energy equation between the lower plenum and the midpoint of the pyrex tube for each channel.

$$x = 1/\left(1 + \frac{\rho_f}{\rho_g}\left(\frac{1-\alpha}{2.649\alpha}\right)1.366\right) \tag{4}$$

Equation (4) is shown in Fig. 7.

Flow Split With One Channel in Cocurrent, and the Other in Countercurrent, Flow. The equations were the same as those for both channels in cocurrent flow, except that for the counter-current channel, the drift flux void fraction equation, with the parameters C_0 and V_{gj} given by the Dix correlation, equation (5) and reference [7], replaced equation (4)

$$C_0 = 1.0 + f_1(\delta)^* f_3(\alpha)/(1 + \mathrm{Re}/4.11^*10^5)^{1/2} \tag{5a}$$

$$V_{gi} = 2.5 f_0(\rho) \text{ ------ for } 0 < \alpha < \alpha_2 \tag{5b}$$

$$V_{gj} = (2.5 + f_4(\mathrm{Re})(\alpha - \alpha_2)/0.1)^* f_0(\rho) \quad \text{for } \alpha_2 < \alpha < \alpha_2 + 0.1 \tag{5c}$$

$$V_{gj} = K_g(1-\alpha)^* f_0(\rho) \text{ --- for } \alpha_2 + 0.1 < \alpha < 1.0 \tag{5d}$$

where

$$\delta = \rho_g/\rho_f \tag{5e}$$

$$f_0(\rho) = (g\sigma(\rho_f - \rho_g)/\rho_f^2)^{1/4} \tag{5f}$$

$$\alpha_2 = 0.625 + 0.15\exp(-\mathrm{Re}/1.12^*10^5) \tag{5g}$$

$$f_1(\delta) = 0.5 \text{ for } \delta << 1.0 \tag{5h}$$

$$K_g = (2.5 + f_4(\mathrm{Re}))\delta^{1/2}/(0.9 - \alpha_2) \tag{5i}$$

$$f_3(\alpha) = 1.0 \text{ for } \alpha \le \alpha_1 \tag{5j}$$

$$= (1.0-\alpha)/(1.0-\alpha_1) \text{ for } \alpha > \alpha_1 \tag{5k}$$

$$\alpha_1 = (5/6)^* f_1(\delta)/(1 + \mathrm{Re}/4.11^*10^5)^{1/2}) \tag{5l}$$

$$f_4(\mathrm{Re}) = 0.9(1 - (\mathrm{Re}/2.01^*10^5)) \quad \mathrm{Re} \le 2.01^*10^5 \tag{5m}$$

$$= 0.0 \quad \mathrm{Re} > 2.01^*10^5 \tag{5n}$$

The above correlation was developed for cocurrent flow. However, by using the absolute value of the Reynolds number, the equation was found to correlate data for chugging counter-current flow well, as shown in Fig. 8. The countercurrent flow regime in the tests were of the chugging type.

Flow Split With One Channel in Cocurrent Flow, and the Other in Single Phase Liquid Downflow. The equations were the same as for the previous flow split cases, except that for the channel with single phase liquid, $W_g = 0$.

Analysis

A simple flow split relationship can be developed for the case in which both the lower plenum and all the channels are in cocurrent upflow. Figure 9(*a*) illustrates such a case. The flow is assumed homogeneous in the lower plenum. If X_0 and P_0 are the quality and pressure in the lower plenum at the flow split elevation, and X_1, P_1, X_2, P_2 are the qualities and pressures at entries to the respective channels, then at steady state,

$$x_0 h_{fg0} + h_{f0} + \frac{V_0^2}{2J} = x_1 h_{fg1} + h_{f1} + \frac{V_1^2}{2J} = x_2 h_{fg2} + h_{f2} + \frac{V_2^2}{2J} \tag{6}$$

If $P_1 \doteq P_2 \doteq P_0$ and kinetic energy changes are negligible, then

$$x_1 = x_2 = x_0 \tag{6a}$$

The flow split relationship for this flow situation becomes

$$x_{ch} = x_{lp} \tag{6b}$$

Figure 9(*b*) illustrates the more complicated case in which one channel is in cocurrent upflow while the other is in countercurrent flow, at their inlets. The inlets of both channels are submerged in the two phase fluid in the lower plenum.

Let W_{gi}, W_{fi} be the vapor and liquid flows through a channel entry.

a_i = Channel flow area at entry
A_i = Cross sectional area of the stream tube, in the lower plenum at the flow split elevation, through which the flows W_{gi} and W_{fi} pass.
α_i, ϕ_i = average void fractions over a_i and A_i, respectively

From the drift flux equations:

$$\alpha_i \equiv W_{gi} / \left(C_{0i} \left(W_{gi} \pm W_{fi} \frac{\rho_{gi}}{\rho_{fi}} \right) + a_i \rho_{gi} V_{gji} \right) \tag{7}$$

$$\phi_i = W_{gi} / \left(C'_{0i} \left(W_{gi} \pm W_{fi} \frac{\rho'_{gi}}{\rho'_{fi}} \right) + A_i \rho'_{gi} V'_{gji} \right) \tag{8}$$

(the primed quantities refer to values at A_i)

and making the following assumptions:

(*a*) Dynamic pressure heads are negligible, i.e., $P_i = P'_i$

(*b*) $C_0 = C'_0(c) V_{gji} = V'_{gji}$

Then

$$\frac{1}{\alpha_i} = C'_{0i} \left(1 \pm \frac{W_{fi}}{W_{gi}} \frac{\rho_{gi}}{\rho'_{fi}} \right) + a_i \left(\rho'_{gi} \frac{V'_{gji}}{W_{gi}} \right) \tag{9}$$

$$\frac{1}{\phi_i} = C'_{0i} \left(1 \pm \frac{W_{fi}}{W_{gi}} \frac{\rho'_{gi}}{\rho'_{fi}} + A_i \left(\rho'_{gi} \frac{V'_{gji}}{W_{gi}} \right) \right) \tag{10}$$

$$\frac{1}{\phi_i} - \frac{1}{\alpha_i} = \frac{\rho'_{gi} V'_{gji}}{W_{gi}/A_i} \left(1 - \frac{a_i}{A_i} \right) \tag{11}$$

If, as in many cases of practical application, $a_i << A_i$, then equation (11) becomes

$$\frac{1}{\phi_i} - \frac{1}{\alpha_i} = \frac{\rho'_{gi} V'_{gji}}{W_{gi}/A_i} \tag{12}$$

Equation (11) has the correct limit as a_i approaches A_i. If we assume that both the void fraction and the vapor flux are uniform across a given elevation in the lower plenum, then

$$\phi_i = \alpha_{lp} \text{ at the flow split elevation} \tag{13}$$

$$W_{gi}/A_i = (W_g/A)_{lp} \text{ " " "} \tag{14}$$

When the void distribution over a lower plenum elevation is uniform, equations (13) and (14) are compatible. Such a situation is approximated during bulk vaporization in the lower plenum of a nuclear reactor which is undergoing a depressurization transient, or when all the channels and the lower plenum are in cocurrent flow or countercurrent flow. If some channels are in cocurrent flow while others are in countercurrent flow at their inlets, the two equations are not compatible. However, for computational reasons, we may assume the two equations to hold. Equations (11) and (12) then become

$$\frac{1}{\alpha_{lp}} - \frac{1}{\alpha_{ch}} = \left(\frac{\rho_g V_{gj}}{G} \right)_{lp} \left(1 - \frac{a_i}{A_i} \right) \tag{15}$$

$$\frac{1}{\alpha_{lp}} - \frac{1}{\alpha_{ch}} = \left(\frac{\rho_g V_{gi}}{G} \right)_{lp} \tag{16}$$

where lower plenum values are calculated at flow split elevation. When $a_i << A_i$, as will be the case if the channel inlet area is a significant proportion of the total lower plenum cross-sectional area at the flow split elevation, then equation 15 will be used, and the ratio a_i/A_i must be estimated. An estimate for the ratio is obtained by assuming that

$$A_i/A_{lp} = a_i / \sum_i a_i \tag{17}$$

$$\therefore a_i/A_i = \left(\sum_i a_i \right) / A_{lp} \tag{18}$$

Results

Test results for the matrix of Table 1 are shown in Table 2. The flow split data for both the channels and the lower plenum in cocurrent upflow are plotted in Fig. 10 and 11, for the HPT and LPT. Equation (6*b*) is seen to represent the data well, within experimental errors.

Figure 12 shows a plot of $(1/\alpha_{lp} - 1/\alpha_{ch})$ versus $(\rho_g V_{gj}/G_g)_{lp}$ for all the flow split combinations observed. Within the channels themselves, the observed flow regimes were churn-turbulent or slug or anular for cocurrent flow, chugging countercurrent flow, or single phase liquid downflow. Channel inlet void fractions when in countercurrent flow, V_{gj} and lower plenum void fractions were calculated using the Dix correlation (equation (5)). The figure also shows a comparison of the data with equation (16). The data are biased to one side of the equation, but nevertheless, the comparison is quite good.

The data in figure 12 appears to follow the equation

$$1/\alpha_{lp} - 1/\alpha_{ch} = \Phi + (\rho_g V_{gj}/G_g)_{lp} \tag{19}$$

Φ is non zero if the first two terms on the right-hand side of equations (9) and (10), or V_{gj} and V'_{gj} and V'_{gj}, are not equal. It is therefore a measure of how accurate assumptions (*a*), (*b*), and (*c*), on which the equations were based, are.

For the tests reported here, the maximum dynamic pressure head at channel entry was estimated as 4 percent of lower plenum pressure. This would introduce less than a 5 percent difference in vapor density, and negligible difference in liquid density. At rated flows, the dynamic pressure head at the channel entry nose piece of a BWR is 0.2 percent to 0.27 percent of system pressure (69 bar). Thus assumption (*a*) is fairly good.

Using the Dix correlation (equation (5)), the ratios C_0/C'_0 and V_{gj}/V'_{gj} were determined for $0.01 < \phi < 0.7$; $10^3 \le R'_e \le 10^5$; $1.01 \le P \le 69$ bar and $0.0 < a_i/A_i \le 1$. It was found that within these ranges of parameters, $0.8 \le C_0/C'_0 \le 1.0$. The V_{gj}-ratio was less well behaved. However, for $a_i/A_i > 0.5$ and $Re = 10^5$, then $0.8 < V_{gi}/V'_{gj} < 1.1$. For $a_i/A_i > 0.2$ and $Re = 10^3$, then $0.8 < V_{gj}/V'_{gj} < 1.3$. Assumption (*b*) is therefore acceptable within the range of parameters given above. Assumption (*c*) is admissible for $\phi < 0.7$, $a_i/A_i > 0.3$ and $10^3 \le R'_e \le 10^5$.

The data plotted in Figs. 10, 11, 12 were obtained with various test-section power levels, within the range given in the test matrix. No definite effect of channel power level or power ratio was observed in the figures.

For the tests with zero net liquid flow rate, the method of introducing the vapor into the channels was varied between a gradual and a sudden introduction of vapor. With gradual increase in vapor flow rate, the LPT remained in single phase liquid downflow until a total vapor flow rate of 0.0114 kg/s was reached. Chugging countercurrent flow was then established in this channel. On reduction of total vapor flow

rate, single phase liquid downflow was not re-established in this channel until the vapor flow rate was reduced to 0.0058 kg/s. There was thus a hysteresis effect on the flow configuration obtained as the total vapor flow rate was varied. It was also found that with sudden addition of vapor, chugging countercurrent flow was established in the LPT provided the total vapor flow rate was greater than 0.0058 kg/s. In all these flow configuration tests with zero net liquid flow, the HPT was in cocurrent upflow.

Figure 12 includes data obtained from the above flow configuration tests. Thus, though the method of introducing the flows affected the resulting flow configuration, the stable flow split relationship was not affected.

Conclusions

1. Simple flow split relationships for channels communicating between the same upper and lower plena have been developed and are given by equations (6*b*) and (15) or (16).

2. Equation (6*b*) is applicable when the lower plenum and all the channel inlets are in cocurrent upflow, and the lower plenum void distribution is uniform at a given elevation.

3. Equation (15) or (16) is applicable when the channel entries are submerged in a two-phase flow in the lower plenum, and the channel in question is in two phase flow at its lower plenum entry. The following conditions also need to be satisfied.

(*a*) Uniform void distribution in the lower plenum at the flow split evaluation.
(*b*) Low void fractions in the lower plenum (<0.7)
(*c*) Moderate-to-high ratio of total channel inlet areas to lower plenum cross-sectional area at flow split elevation.
(*d*) $10^3 \leq (\mathrm{Re})_{lp} \leq 10^5$. (The validity of the assumption on which the relationship was developed was not tested for $\mathrm{Re}_{lp} > 10^5$)

4. Experimental data from a vertical two channel system at near atmospheric pressure, have been compared with the relationships, with encouragingly good results.

5. Within the range of channel power levels and power ratios tested, no effect of these parameters was found to influence the validity of the flow split correlations.

6. Though the method of introducing the flows, and the flow levels, may influence the modes of flows at the channel entries, once a flow configuration is known to exit, equation (6*b*) or (15) or (16) will apply, irrespective of how the flows were established.

References

1 Eselgroth, P. W., and Griffith, P., "Natural Convection Flows in Parallel Connected Vertical Channels With Boiling," M.I.T. Report No. 70318-49, July 1967.

2 Iloeje, O. C., "Effects of Parallel Channel Interactions, Steam Flow, Liquid Subcool, and Channel Heat Addition on Nuclear Reactor Reflood Transient." (to be published) *Nigerian J. of Tech.*, NIJOTECH, Sept. 1982.

3 Eselgroth, P. W., and Griffith, P., "The Prediction of Multiple Heated Channel Patterns From Single Channel Pressure Drop Data," M.I.T. Report No. 70318-57, Oct. 1968.

4 Iloeje, O. C., and Avila, J., "Two Phase Flow Split Model For Parallel Channels," *Nig. J. of Tech.* (NIJOTECH), Mar. 1979.

5 Iloeje, O. C., Kervinen, J., Ireland, J., and Shiralrar, B. S., "Two Phase Flow Configurations and Flow Splits in Parallet Channels," General Electric Nuclear Energy Division, San Jose, NEDE, 1977.

6 Latzko, H., Z. angew Math. U. Mech., Vol. 1, p. 227, 1921; and as in *Turbulence*, by Hinze, J. O., p. 514, McGraw-Hill Book Co., 1959.

7 Dix, G. E., Sursock, J. P., and Wing, K. D., "New BWR Void Fraction Correlation," BWR Systems Department, Gen. Elec. Nuclear Energy Div., San Jose, Calif., Aug. 1975.